Elastic properties of Nb-based alloys by using the density functional theory*

Liu Zeng-Hui(刘增辉) and Shang Jia-Xiang (尚家香)†

School of Materials Science and Engineering, Beihang University, Beijing 100191, *China*

(Received 29 October 2010; revised manuscript received 24 June 2011)

A first-principles density functional approach is used to study the electronic and the elastic properties of $Nb_{15}X$ (X = Ti, Zr, Hf, V, Ta, Cr, Mo, and W) alloys. The elastic constants c_{11} and c_{12}, the shear modulus C', and the elastic modulus $E_{\langle 100\rangle}$ are found to exhibit similar tendencies, each as a function of valence electron number per atom (EPA), while c_{44} seems unclear. Both c_{11} and c_{12} of $Nb_{15}X$ alloys increase monotonically with the increase of EPA. The C' and $E_{\langle 100\rangle}$ also show similar tendencies. The elastic constants (except c_{44}) increase slightly when alloying with neighbours of a higher d-transition series. Our results are supported by the bonding density distribution. When solute atoms change from Ti(Zr, Hf) to V(Ta) then to Cr(Mo, W), the bonding electron density between the central solute atom and its first neighbouring Nb atoms is increased and becomes more anisotropic, which indicates the strong interaction and thus enhances the elastic properties of Nb–Cr(Mo, W) alloys. Under uniaxial ⟨100⟩ tensile loading, alloyed elements with less (more) valence electrons decrease (increase) the ideal tensile strength.

Keywords: Nb-based alloys, elastic properties, density functional calculations

PACS: 62.20.dq, 71.15.Mb **DOI:** 10.1088/1674-1056/21/1/016202

1. Introduction

Niobium (Nb) is one of the most promising refractory metals for future high temperature structural materials due to its high melting point and good room temperature ductility.[1] However, its insufficient high temperature strength is one of its shortcomings. To improve its mechanical properties, solid solution strengthening is always adopted.[2] Solid solution strengthening and creep strength, as well as the fracture transition temperature have been extensively studied in experiment.[3−6] However, for transition metals, it is necessary to understand the intrinsic effects of alloying elements on mechanical properties.

Many studies[7−9] extensively focus on the pure VB family elements due to their elastic, dynamic, and electronic properties. Unlike other bcc metals, Nb(V) will fail under uniaxial tension not by {100} cleavage, but by ⟨111⟩ {112} shear.[9,10] In addition, there is a structural phase transition of V from bcc to a rhombohedral phase at about 63–69 GPa.[11] Theoretical calculations confirmed a pronounced softening of the trigonal shear moduli of V and Nb under compression, driving a mechanical instability of bcc V while the shear modulus of Nb softens for pressures around 50 GPa, but remains positive.[12] The elastic anomaly of Nb is also reflected in an anomaly of the phonon dispersion relation.[13] It is realized that the occurrence of strong softening in the shear modulus and the possibility of an associated rhombohedral phase are not compatible with the traditional view of simple d-electron bonding in transition metals,[14] which is primarily due to the intra-band nesting of the Fermi surface.[12,15]

It is well known that the solid solution strengthening cannot be interpreted solely on the basis of atomic size misfit, but reflects a combination of atomic size and other effects, such as an elastic modulus misfit or solute association effects.[4] Recently, Hideaki *et al.*[16] realized the mechanism of the low elastic modulus of the Ti binary alloys, i.e., the valence electron number per atom (EPA) of Ti binary alloy can be controlled by the quantity of VB or VIB family element, resulting in a low Young's modulus material. At the same time, the effect of alloying on the phase stability of group VB (V, Nb, and Ta) transition metals has been studied by Landa *et al.*[17] and two dominant mechanisms are recognized. The band energy tends to destabilize or stabilize the bcc phase when a particular group VB metal is or is not alloyed with the same *d*-transition series. The elastic constant of Nb alloy is an important parameter which is related to the other mechan-

*Project supported by the National Natural Science Foundation of China (Grant No. 50771004).

†Corresponding author. E-mail: shangjx@buaa.edu.cn

© 2012 Chinese Physical Society and IOP Publishing Ltd

ical properties such as high temperature strength and it is also the input parameter to the finite element analysis calculation as well as developing reliable classical Nb-based alloy potentials for molecular dynamics simulation. In this paper, we aim to investigate the elastic property of solid solution of Nb and to study more generally how it is influenced by alloying with the neighbouring elements in the periodic table.

According to the experimental phase diagram,[18] the Nb and transition metals X (X = Ti, Zr, Hf, V, Ta, Mo and W) each form a bcc solid solution with a large solubility, except for Cr, which forms the Cr_2Nb phase. Since first-principles methods have achieved great success in studying the strengths of materials,[19−21] we apply a density functional theory (DFT) approach in order to provide reliable data to understand the elastic properties of Nb-solid solution systems. Only the simple ordered bcc solid solution is considered in our calculations. The rest of the present paper is organized as follows: after a brief description of the theory and model, the structural and the elastic properties of $Nb_{15}X$ alloys are discussed. To further understand the electronic nature of the mechanical properties in these alloys, the electronic structure, the bonding nature, and the stress strain relation of Nb alloys under tension are analysed. Finally, a short summary is presented in the last section.

2. Computational method and models

In this paper, we study the elastic properties and the ideal tensile strengths of Nb–X solid solution alloys by using DFT, where X = Ti, Zr, Hf, V, Ta, Cr, Mo and W. Supercells each containing 16 atoms ($2 \times 2 \times 2$ cubic cells), with one solute atom at the central site, were used to model the $Nb_{15}X$ solid solution alloys. For all calculations we adopted the Vienna Ab Initio Simulation Package (VASP),[22] making use of the all-electron projector augmented wave method within the generalized gradient approximation of Perdew *et al.*[23] The $2\times2\times2$ supercell calculations were conducted with a $13\times13\times13$ Monckhorst–Pack grid. The plane wave cutoff energy is 550 eV. For the $Nb_{15}Cr$, the spin-polarized calculations were performed, indicating no magnetization on the solute atom, so all simulations were performed without spin polarization. The total energy was calculated with a high accuracy, converged to 10^{-8} eV/atom. The relaxation is done until the force on each atom is less than 0.01 eV/Å.

For a cubic system, the number of the independent elastic constants reduces to three (c_{11}, c_{12}, and c_{44}) due to the symmetry of the crystal. Elastic modulus $C' = (c_{11} - c_{12})/2$ and c_{44} are evaluated from the total energy of the crystal to which volume-conserving orthorhombic and monoclinic distortions have been applied.[7,24] The bulk modulus is determined by fitting the calculated total energy versus the volume to the equation of state (EOS) function.[25] The two cubic elastic constants c_{11} and c_{12} are decoupled using the relation $B_0 = (c_{11} + 2c_{12})/3$. The Young's modulus along the $\langle 100 \rangle$ direction, $E_{\langle 100 \rangle}$, can be obtained from $E_{\langle 100 \rangle} = [(c_{11} - c_{12})(c_{11} + 2c_{12})]/(c_{11} + c_{12})$.[10]

The ideal strength of a material is the minimum stress required to yield or break a perfect crystal. It has been accepted as an essential mechanical parameter of materials. To determine the ideal strength, we adopted the standard approach as described in Ref. [9]. We also calculated the stress strain relation under tensile along the $\langle 100 \rangle$ direction. After obtaining the equilibrium structure, a series of incremental tensile strains was applied to the crystal. To ensure that the material was under a uniaxial stress state, relaxation was performed by keeping the applied strain fixed and adjusting the other two normal strain components independently until the calculated conjugate Hellmann–Feynman stress was less than 0.1 GPa.

3. Results and discussion

3.1. Elastic properties of pure Nb

The calculated lattice parameters, the elastic constants c_{ij}, together with the corresponding results from experiments and previous calculations of pure Nb, are listed in Table 1. The calculated lattice parameters show good agreement with the experimental results. The calculated elastic constants c_{11} and c_{12} of Nb are close to the experimental values, whereas c_{44} shows a significant underestimate with respect to

Table 1. Values of lattice parameter a, bulk modulus B_0 and the elastic constant c_{ij} of pure Nb compared with the experimental results.

Source	a/Å	B_0/GPa	c_{11}/GPa	c_{12}/GPa	c_{44}/GPa
This study	3.309	171.3	247.8	133.1	17.2
Theory[12]	3.322	174.3	247	138	10.3
Theory[16]	3.325	171.7	247	134	15.6
Experiment[26]	3.307	171.8	246.5	134.5	28.7

the experimental value. This result is similar to the other calculated results.[7,12,16] The theoretical underestimation of the c_{44} elastic constant of Nb at ambient pressure is probably related to the nesting properties of the Fermi surface which produce a van Hove singularity in the electronic density of the state close to the Fermi level.[10,12]

3.2. Elastic properties of $Nb_{15}X$

Table 2 shows the calculated lattice parameters, bulk modulus, elastic constants c_{ij}, shear modulus C', Young modulus $E_{\langle 100\rangle}$, and EPA of $Nb_{15}X$ alloys for different doped elements, where X = IVB: Ti, Zr, Hf; VB: V, Ta; VIB: Cr, Mo, W. For the Ti, Zr and Hf doping alloys of IVB metals, the bulk moduli of Nb_{15}Ti(Zr, Hf) are decreased, which is in contrast to the VIB metals Cr, Mo and W doping, the bulk moduli of the Nb_{15}Mo(Cr,W) alloys are increased, while those of the Nb_{15}V(Ta) alloys change slightly. This indicates that the EPA plays an important role in bulk modulus. This tendency is very similar to that of the bulk modulus result of M_2AC (M = Ti, Zr, Hf, V, Nb, Ta, Cr, Mo, W and A = Al, Ga, Ge, Sn).[27] The Ti_2(Zr, Hf)AC was found to have lower bulk moduli than other doped materials.

The elastic constants c_{11}, c_{12}, C' as well as the elastic modulus $E_{\langle 100\rangle}$ are found to exhibit similar tendencies, each is a function of EPA. These elastic moduli of $Nb_{15}X$ alloys increase when EPA changes from 4.93 to 5.06. It is clear that both c_{11} and c_{12} of $Nb_{15}X$ alloys increase monotonically with the increase of EPA, and C' and $E_{\langle 100\rangle}$ show similar tendencies. When a certain EPA value is given, the elastic constant (except c_{44}) changes slightly when alloying with neighbours of higher d-transition series. Compared with the data of pure Nb alloy, the c_{11}, c_{12} and $E_{\langle 100\rangle}$ of IVB elements (Ti, Zr and Hf) decrease, while those of VIB elements increase. The calculated c_{44} of $Nb_{15}X$ is very low, and its relation with the valence electron number is not clear. It seems that c_{44} is determined not only by the valence electron number per atom but also by the other parameters, which is similar to that of Ti alloys.[16]

3.3. Density of states (DOS)

The change in elastic property of an alloy originates from the variation of electronic structure. We chose the typical Hf, Ta and W doping elements to represent the IVB, VB and VIB metals doping, respectively. Figure 1 shows the calculated partial densities of states (PDOS) of the Nb_{15}Hf, Nb_{15}Ta and Nb_{15}W, respectively. Only the PDOSs of the central doping metal atom and their first nearest-neighbour Nb atom are shown.

The Ta-d orbital and Nb-d orbital overlap each other, and the Hf-d peaks are lower than the Nb-d peaks while W-d peaks are higher. This feature of d-DOSs can be understood by the different valence electron numbers of elements. For Nb_{15}W, W has one more valence electron than Nb according to the electron configuration. The excess valence electrons contribute to the W-d, p and s orbitals. Thus, there are strong interactions between W and Nb atoms through d–d hybridization. However, for Nb_{15}Hf, the Hf-d orbital is lower than Nb-d orbital and the interaction between Hf and Nb becomes weak. There are similar situations for other transition metals.

By analysing the above results, we suggest the valence electron number has main influence on the behaviour of elastic constant. Either the decrease or the increase of the electron number affects the interatomic bonding which should play a main role in solid solution strengthening.

Table 2. Values of lattice parameter, bulk modulus B_0, the elastic constant c_{ij}, shear modulus C', Young's modulus $E_{\langle 100\rangle}$ of $Nb_{15}X$, and EPA.

Alloys	$2a$/Å	B_0/GPa	c_{11}/GPa	c_{12}/GPa	c_{44}/GPa	C'/GPa	$E_{\langle 100\rangle}$/GPa	EPA
Nb_{15}Ti	6.609	166.4	239.2	130	17.7	54.6	147.7	
Nb_{15}Zr	6.650	163.5	232.8	128.8	15.1	52	141.0	4.93
Nb_{15}Hf	6.645	165.1	234.8	130.3	17.9	52.3	141.8	
Nb_{15}V	6.585	171.2	246.7	133.4	16.8	56.7	153.1	
Pure Nb	6.618	171.3	247.8	133.1	17.2	57.3	154.8	5.0
Nb_{15}Ta	6.619	172.7	249.8	134.2	20.4	57.8	155.9	
Nb_{15}Cr	6.569	173.6	248.7	136.1	11.9	56.3	152.2	
Nb_{15}Mo	6.595	176.2	253.3	137.6	12.0	57.8	156.4	5.06
Nb_{15}W	6.599	177.7	256.4	138.3	17.9	59.1	159.4	

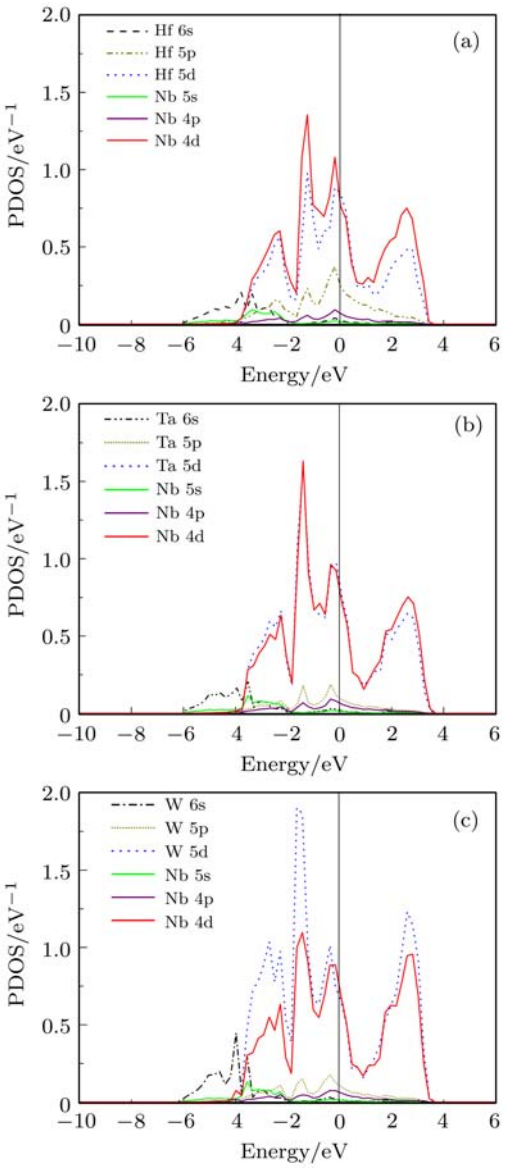


Fig. 1. (colour online) Calculated partial densities of states (PDOS) of $Nb_{15}X$: (a) $Nb_{15}Hf$, (b) $Nb_{15}Ta$, and (c) $Nb_{15}W$. The vertical line denotes the Fermi energy.

Comparing the PDOSs of $Nb_{15}Hf$, $Nb_{15}Ta$ and $Nb_{15}W$, it can be found that the energy peaks of $Nb_{15}W$ are shifted toward the low energy levels and those of $Nb_{15}Hf$ toward the high energy levels compared with those of pure Nb system. Considering the valence electron number and PDOS, it can be obtained that IVB metals (Ti, Zr, Hf) destabilize metal Nb and that VIB metals Cr, Mo and W would stabilize it, which are similar to the results of phase stability of vanadium with Madelung and band energy effects due to alloying.[17,28]

3.4. Bonding density distribution

In order to show the bonding characteristic in $Nb_{15}X$ alloy more visually, we calculate the bonding charge distribution. The bonding charge distribution is the difference between the self-consistent charge distribution from a first-principles DFT calculation and the superposition of atom charge densities of the individual atoms.[29] The bonding density distribution is plotted by using VESTA.[30] Figure 2 shows the bonding charge densities in the (110) planes of various alloys. The region with a higher charge density indicates stronger bond formation in the region. In each plot the doped element atom is at the central position. The colour indicates bonding charge value; red denotes an increase of accumulated charge (i.e. an increase in the electron density) after bonding, deep blue indicates a charge density loss.

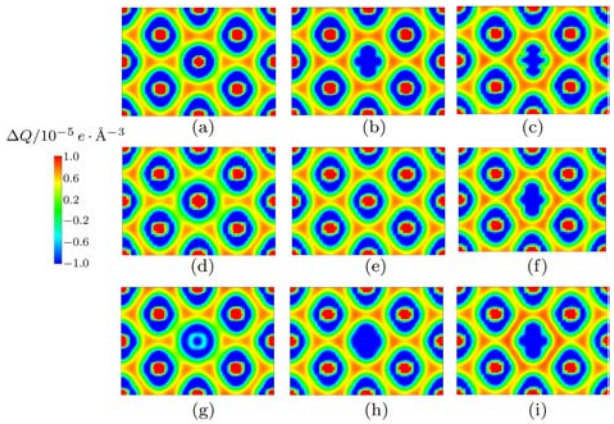


Fig. 2. (colour online) Bonding density distributions of $Nb_{15}X$ on the (110) (ΔQ is the charge density difference, and e is the charge of one electron). The solute atom is in the centre of each plot and is surrounded by Nb atoms. Red means an increase of the charge accumulated, deep blue means a charge density loss. (a) $Nb_{15}Ti$, (b) $Nb_{15}V$, (c) $Nb_{15}Cr$, (d) $Nb_{15}Zr$, (e) pure Nb (f) $Nb_{15}Mo$, (g) $Nb_{15}Hf$, (h) $Nb_{15}Ta$, (i) $Nb_{15}W$.

It is shown that the different solute elements in the $Nb_{15}X$ alloys cannot change the Nb–Nb bonding characteristic and only affect the Nb–X bonding characteristic. Also from our structural relaxation, most of the relaxation occurs in the first nearest-neighbour shell around solute atom, indicating that effects are localized around each solute atom. When the doping elements change from Ti(Zr, Hf) to V(Ta) then to Cr(Mo, W), the distribution of bonding charge density around X changes from isotropic to anisotropic, then to more anisotropic. The distribution of bonding charge density around IVB elements Ti, Zr and Hf is isotropic(i.e., s-orbit like), whereas the directional d bond characteristic is clearly seen for alloys with the VIB transition elements Cr, Mo and W. In addition, the bonding charge density between Nb and V (or Ta) is similar to that of pure Nb. When solute atoms change from Ti(Zr, Hf) to V(Ta) then to Cr(Mo, W),

the bonding electron density between the central solute atom and its first neighbouring Nb atoms is increased, and more charges are located around the Nb–Cr(Mo, W) bonds, which indicates that the strong interaction is increased and thus the elastic properties of Nb–Cr(Mo, W) alloy are enhanced. The more isotropic bonding characteristics (i.e. s-orbit like) in the $Nb_{15}Ti(Zr, Hf)$ alloys account for the lower elastic modulus.

The charge redistribution provides us with a clear picture of electronic structure origin, i.e., the intrinsic effect of alloying elements on the mechanical properties.

3.5. Tensile strength calculation

The elastic constants obtained strictly within the linear elasticity regime of a material cannot give an accurate account for the material strength under a larger strain. The ideal tensile strength of a bcc metal is expected to have its minimum value for tensile in the ⟨001⟩ direction. We therefore calculate the stress-strain curve of Nb–X alloys for this case. The stress-strain curves for $Nb_{15}X$ along the ⟨001⟩ direction are shown in Fig. 3. The stress increases monotonically as the strain increases and reaches its maximum value at a strain of about 0.18. For pure Nb, the value of the maximum stress is 17.2 GPa, which is close to the results of Ref. [9]. The ideal tensile strength of $Nb_{15}Mo(W)$ is higher, and that of $Nb_{15}Cr(V, Ta)$ is slightly lower than that of pure Nb, whereas the tensile strength of $Nb_{15}Ti(Zr, Hf)$ is much lower than that of pure Nb metal. In addition, from the elastic part (i.e., under a small strain) of the stress-strain curves, the obtained Young's moduli are in excellent agreement with those calculated from single crystal elastic constants.

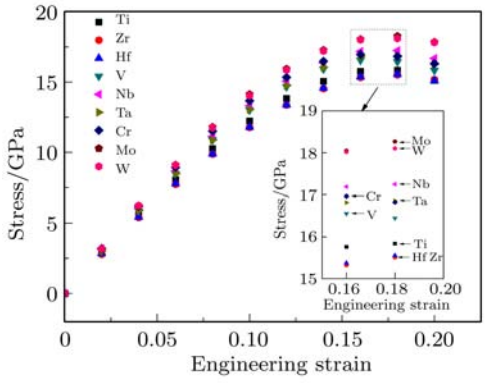


Fig. 3. (colour online) The stress-strain relationships for $Nb_{15}X$ along ⟨100⟩. The inset magnifies the changes in the vicinity of the maximum stress.

4. Conclusion

We calculate the elastic properties and ideal tensile strengths of $Nb_{15}X$ alloys (X = Ti, Zr, Hf, V, Ta, Cr, Mo and W) by using DFT. Both c_{11} and c_{12} of $Nb_{15}X$ alloys increase monotonically with the increase of EPA. The C' and $E_{\langle 100\rangle}$ also show similar tendencies. The elastic constants (except c_{44}) increase slightly when alloying with neighbours of higher d-transition series. The observed relationship between elastic constant and doped element is explained as a result of the valence electron concentration. When EPA changes from 4.93 to 5.06, the distribution of bonding charge density around X changes from isotropic to more anisotropic. It is shown that the observed directional bonding for alloying in Nb-based alloys doped by VIB elements can enhance the ideal tensile strength and increase the elastic constants.

References

[1] Slining J R and Koss D A 1973 *Metall. Trans.* **4** 1261
[2] Tabaru T, Kim J H, Shobu K, Sakamoto M, Hirai H and Hanada S 2005 *Metall. Mater. Trans.* **36** 617
[3] Koss D A 1971 *Metall. Trans.* **2** 245
[4] Klein M J and Metcalfe A G 1973 *Metall. Trans.* **4** 2441
[5] Rosenberg H W and Nix W D 1972 *Metall. Trans.* **4** 1333
[6] Peters B C and Hendrickson A A 1970 *Metall. Trans.* **1** 2271
[7] Söderlind Per, Eriksson Olle, Wills J M and Boring A M 1993 *Phys. Rev.* B **48** 5844
[8] Grad G B, Blaha P, Luitz J, Schwarz K, Fernández Guillermet A and Sferco S J 2000 *Phys. Rev.* B **62** 12743
[9] Luo W D, Roundy D, Cohen, Marvin L and Morris J W 2002 *Phys. Rev.* B **66** 094110
[10] Nagasako N, Jahnátek M, Asahi R and Hafner J 2010 *Phys. Rev.* B **81** 094108
[11] Ding Y, Ahuja R, Shu J F, Chow P Luo W and Mao H K 2007 *Phys. Rev. Lett.* **98** 085502
[12] Koči L, Ma Y, Oganov A R, Souvatzis P and Ahuja R 2008 *Phys. Rev.* B **77** 214101
[13] Nakagawa Y and Woods A D B 1963 *Phys. Rev. Lett.* **11** 271
[14] Skriver and Hans L 1985 *Phys. Rev.* B **31** 1909
[15] Landa A, Klepeis J, Söderlind P, Naumov I, Velikokhatnyi O, Vitos L and Ruban A 2006 *J. Phys. Conden. Matter* **18** 5079
[16] Hideaki I, Nagasako N, Tadahiko F, Atsuo F, Kazutoshi M and Takashi S 2004 *Phys. Rev.* B **70** 174113
[17] Landa A, Söderlind P, Ruban A V, Peil O E and Vitos L 2009 *Phys. Rev. Lett.* **103** 235501
[18] http://www.crct.polymtl.ca/fact/documentation/SGTE/
[19] Liu N N, Song R B and Du D W 2009 *Chin. Phys.* B **18** 1979
[20] Zhu J, Yu J X, Wang Y J, Chen X R and Jing F Q 2008 *Chin. Phys.* B **17** 2216

[21] Zhou J J, Chen Y G,Wu C L, Pang L J, Zheng X and Gao T 2009 *Acta Phys. Sin.* **58** 7044 (in Chinese)

[22] Kresse G and Furthmüller J 1996 *Phys. Rev.* B **54** 11169

[23] Perdew, John P, Burke K and Ernzerhof M 1996 *Phys. Rev. Lett.* **77** 3865

[24] Bleskov I D, Smirnova E A, Vekilov Y K, Korzhavyi P A, Johansson B, Katsnelson M, Vitos L, Abrikosov I A and Isaev E I 2009 *Appl. Phys. Lett.* **94** 161901

[25] Birch F 1947 *Phys. Rev.* **71** 809

[26] Trivisonno J, Vatanayon S, Wilt M, Washick J and Reifenberger R 1973 *J. Low Temper. Phys.* **12** 153

[27] Sun Z M, Denis M, Rajeev A, Sa L, Schneider J M 2004 *Phys. Rev.* B **70** 092102

[28] Delaire O and Fultz B 2006 *Phys. Rev. Lett.* **97** 245701

[29] Gschneidner Jr K A, Min J, Wang C Z, Ho K M, Russell A M, Mudryk Y, Becker A T and Larson J L 2009 *Acta Mater.* **57** 5876

[30] Momma, Koichi and Izumi F 2008 *J. Appl. Crystallog.* **41** 653